International Journal of Medical and Pharmaceutical Research

Online ISSN-2958-3683 | Print ISSN-2958-3675
Frequency: Bi-Monthly
Available online on: https://ijmpr.in/

Original Article

In Silico 2D-QSAR Modeling and Molecular Docking Analysis of Benzylidene-Derived Analogs as 17β-Hydroxysteroid Dehydrogenase Type 3 Inhibitors

Sam Jeffrey B. Tiongco[1*], Russel Joshua L. Sabado[2], Justine De Vera Aquino[1], Bai Gwyneth B. Mamenting[3], Bea Rheena V. Pascual[1], Diana Lorraine G. Salomon[1], Aron Miguel A. Espiritu[1]

[1]Saint Louis University – School of Medicine, Baguio City, Philippines
[2]University of the East Ramon Magsaysay – College of Medicine, Quezon City, Philippines
[3]Cagayan State University – College of Medicine, Tuguegarao City, Philippines

OPEN ACCESS

Corresponding Author:

Sam Jeffrey B. Tiongco
Saint Louis University – School of Medicine, Baguio City, Philippines
Email:
samjeffreybitaotiongco@gmail.com

Received: 16-04-2026
Accepted: 09-05-2026
Available online: 15-05-2026

ABSTRACT

Background: Prostate cancer progression is partly driven by androgenic stimulation, particularly through testosterone and dihydrotestosterone. Inhibition of 17β-hydroxysteroid dehydrogenase type 3, an enzyme involved in testosterone biosynthesis, has emerged as a potential strategy for identifying novel anti-androgenic agents.
Aim: This study aimed to develop and validate an in silico 2D quantitative structure-activity relationship model for benzylidene-derived analogs as potential 17β-hydroxysteroid dehydrogenase type 3 inhibitors.
Methodology: A dataset of 49 benzylidene-derived analogs with reported inhibitory activity against 17β-hydroxysteroid dehydrogenase type 3 was used. Molecular descriptors were computed and pretreated before model generation. A genetic algorithm-based multilinear regression model was developed and validated using internal, external, robustness, y-randomization, and applicability domain analyses. Molecular docking was performed to support descriptor-based mechanistic interpretation.
Results: The best genetic algorithm-multilinear regression model contained eight molecular descriptors and showed good statistical performance, with $R^2 = 0.8994$, $Q^2LOO = 0.8366$, $R^2PRED = 0.8792$, and RMSEP = 1.1709. The model passed internal and external validation criteria, showed robustness in leave-N-out cross-validation, and demonstrated low probability of chance correlation based on y-randomization. Applicability domain analysis showed that all training and test compounds were within the model domain, while seven of eight true external compounds yielded reliable predictions. Mechanistic interpretation suggested that inhibitory activity was mainly influenced by descriptors related to atomic polarizability, hydrophobicity, and electrospatial topology.
Conclusion: The validated 2D-QSAR model, supported by molecular docking, may serve as a useful computational tool for virtual screening and rational design of benzylidene-derived 17β-hydroxysteroid dehydrogenase type 3 inhibitors for prostate cancer-related drug discovery.

Keywords*: 17β-HSD3; 2D-QSAR; molecular docking; applicability domain.*

INTRODUCTION

Prostate cancer remains one of the most common malignancies affecting men worldwide and continues to contribute substantially to cancer-related morbidity and mortality. Its progression is strongly influenced by androgenic stimulation, particularly through testosterone and dihydrotestosterone, which promote the growth and survival of androgen-dependent prostate cancer cells (Rawla, 2019; Cheng et al., 2020). Although current treatment strategies, including surgery, radiation

therapy, chemotherapy, and androgen deprivation therapy, have improved clinical outcomes, advanced prostate cancer remains difficult to manage because of recurrence, treatment resistance, and adverse effects associated with systemic androgen suppression (Michaelson et al., 2008; Litwin & Tan, 2017).

A key enzyme involved in androgen biosynthesis is 17β-hydroxysteroid dehydrogenase type 3, which catalyzes the reduction of androstenedione to testosterone using NADPH as a cofactor (Harada et al., 2012). Compared with other members of the 17β-hydroxysteroid dehydrogenase family, 17β-hydroxysteroid dehydrogenase type 3 has a more restricted tissue distribution and is primarily expressed in the testes and prostate cancer cells (George et al., 2010; Ning et al., 2017). This makes it an attractive molecular target for the development of selective inhibitors that may reduce androgen production while minimizing off-target hormonal effects. However, the development of such inhibitors remains challenging because therapeutic candidates must demonstrate adequate potency, selectivity, and favorable molecular interactions with the target enzyme.

Several studies have explored 17β-hydroxysteroid dehydrogenase type 3 as a therapeutic target in hormone-dependent prostate cancer. Steroidal and nonsteroidal inhibitors have been investigated, including benzylidene-derived analogs with reported in vitro inhibitory activity (Spires et al., 2005; Vicker et al., 2009; Harada et al., 2012). Despite these efforts, available computational studies that quantitatively relate the structural properties of benzylidene-derived analogs to their inhibitory activity remain limited. In particular, only a few quantitative structure-activity relationship studies have examined this compound class in relation to 17β-hydroxysteroid dehydrogenase type 3 inhibition (Martins & Melo, 2019). This gap limits the ability to rationally identify structural features that may enhance inhibitory activity and support the design of new analogs.

Quantitative structure-activity relationship modeling offers a useful in silico approach for correlating molecular structure with biological activity. By converting chemical structures into numerical molecular descriptors, QSAR models can identify physicochemical and topological properties associated with bioactivity and can be used to predict the activity of structurally related compounds (Tropsha, 2010; Puzyn et al., 2010). When supported by appropriate internal and external validation, applicability domain analysis, and mechanistic interpretation, QSAR models can serve as valuable tools for virtual screening and early-stage drug discovery. Molecular docking can further support QSAR interpretation by providing structural insight into possible ligand-enzyme interactions.

In this study, an in silico 2D-QSAR model was developed using benzylidene-derived analogs with reported inhibitory activity against 17β-hydroxysteroid dehydrogenase type 3. A genetic algorithm-based multilinear regression approach was used to identify molecular descriptors associated with inhibitory activity, and the resulting model was evaluated using internal validation, external validation, robustness testing, y-randomization, and applicability domain analysis. Molecular docking was also performed to support the mechanistic interpretation of descriptor contributions.

The scope of this work was limited to the computational modeling of selected benzylidene-derived analogs as potential 17β-hydroxysteroid dehydrogenase type 3 inhibitors. Toxicological, pharmacokinetic, and experimental biological validation were not performed. Nevertheless, the study provides a validated and mechanistically interpreted computational model that may support virtual screening and rational design of structurally related inhibitors for prostate cancer-related drug discovery.

MATERIALS AND METHODS

2.1 Study Design and Computational Workflow

This study employed an in silico quantitative structure-activity relationship (QSAR) and molecular docking approach to evaluate benzylidene-derived analogs as potential inhibitors of 17β-hydroxysteroid dehydrogenase type 3. The workflow involved dataset preparation, ligand structure generation, descriptor computation, data pretreatment, training and test set division, genetic algorithm-based multilinear regression modeling, model validation, applicability domain analysis, true external prediction, and molecular docking. The general computational workflow is summarized in Figure 1.

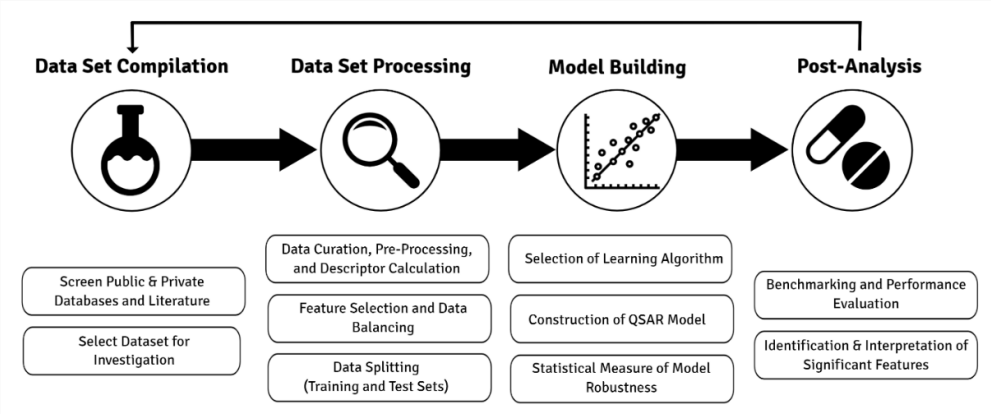

Fig. 1. General workflow for in silico 2D-QSAR modeling and molecular docking analysis. The workflow included dataset collection, ligand preparation, molecular descriptor computation, data pretreatment, dataset division, GA-MLR model generation, internal and external validation, applicability domain analysis, true external prediction, molecular docking, and mechanistic interpretation.

All computations were performed using a Windows 10 operating system with a 64-bit architecture, 16.0 GB RAM, and an Intel Core i7-6700HQ CPU. The software and web-based tools used in the study included MolView for ligand structure generation, Open Babel version 3.1.1 for file conversion, ChemDes for molecular descriptor computation, Data Pretreatment GUI version 1.2 for descriptor filtering, Dataset Division GUI version 1.0 for training and test set division, DTC-QSAR version 1.0.5 for model generation and validation, Prediction Reliability Indicator version 1.0 for true external prediction, Swiss-Model for homology model reconstruction, AutoDockTools version 1.5.6 for molecular docking preparation and simulation, and Protein-Ligand Interaction Profiler for post-docking interaction analysis. Unless otherwise stated, default software settings were used throughout the computational workflow.

2.2 Dataset Collection and Biological Activity

The dataset consisted of 49 benzylidene-derived analogs with reported in vitro inhibitory activity against 17β-hydroxysteroid dehydrogenase type 3. The dataset used in this study was obtained from previously published data by Harada et al. (2012). Additional computed descriptors and validation outputs are available from the corresponding author upon reasonable request. The half-maximal inhibitory concentration values, expressed in nanomolar, were converted to pIC_{50} values using Equation 1 to improve linearity for QSAR modeling. Compounds were included if their inhibitory activity was reported in nanomolar and if they had pIC_{50} values of at least 6.0, which was used as the cutoff for active compounds. Compounds that did not satisfy these criteria were excluded.

$$pIC50 = -\log10(IC50) \quad (1)$$

The structures and biological activity values of the selected analogs are shown in Table 1. The table is placed after the description of dataset selection to allow direct reference to the compounds used in model generation.

Table 1. Structures and inhibitory activities of benzylidene-derived analogs against 17β-hydroxysteroid dehydrogenase type 3.

No.	R1b	R2b	R3	X1	X2	pIC50
	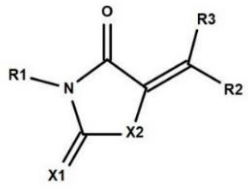					
1	4-OCH3-Ph-	3-Br–4-OH–Ph–	H	S	S	7.85
2	CH3	3-Br–4-OH–Ph–	H	S	S	6.05
3	H2C=CH-CH2-R	3-Br–4-OH–Ph–	H	S	S	6.92
4	HC≡C-CH2-R	3-Br–4-OH–Ph–	H	S	S	6.52
5	CH3OCH2CH2	3-Br–4-OH–Ph–	H	S	S	6.72
6	C6H11	3-Br–4-OH–Ph–	H	S	S	8.52
7	tetrahydropyran-4-yl	3-Br–4-OH–Ph–	H	S	S	7.12
8	4-OCH3-Ph-	3-Br–4-OH–Ph–	H	S	O	7.89
9	Ph-	3-Br–4-OH–Ph–	H	S	O	8.22
10	3-OCH3-Ph-	3-Br–4-OH–Ph–	H	S	O	8.15

11	2-OCH3-Ph-	3-Br–4-OH–Ph–	H	S	O	7.22
12	3,4-OCH2O-Ph-	3-Br–4-OH–Ph–	H	S	O	8.10
13	4-F-Ph	3-Br–4-OH–Ph–	H	S	O	8.70
14	4-Cl-Ph	3-Br–4-OH–Ph–	H	S	O	8.22
15	4-CH3-Ph	3-Br–4-OH–Ph–	H	S	O	8.70
16	4-CF3-Ph-	3-Br–4-OH–Ph–	H	S	O	8.52
17	4-CN-Ph-	3-Br–4-OH–Ph–	H	S	O	7.72
18	4-OCH3-Ph-	3-Br–4-OH–Ph–	H	O	O	7.64
19	4-COOCH3–Ph–	3-Br–4-OH–Ph–	H	O	O	7.62
20	4-C(O)NHCH3–Ph–	3-Br–4-OH–Ph–	H	O	O	7.25
21	4-C(O)N(CH3)2–Ph–	3-Br–4-OH–Ph–	H	O	O	7.60
22	4-C(O)–piperidine–Ph–	3-Br–4-OH–Ph–	H	O	O	7.38
23	4-C(O)–morpholine–Ph–	3-Br–4-OH–Ph–	H	O	O	6.52
24	4-N(CH3)2–Ph–	3-Br–4-OH–Ph–	H	O	O	7.60
25	4-NHAc–Ph–	3-Br–4-OH–Ph–	H	O	O	7.24
26	4-SCH3–Ph–	3-Br–4-OH–Ph–	H	O	O	7.05
27	4-SO2CH3–Ph–	3-Br–4-OH–Ph–	H	O	O	6.05
28	pyridin-2-yl	3-Br–4-OH–Ph–	H	O	O	7.13
29	pyridin-3-yl	3-Br–4-OH–Ph–	H	O	O	7.67
30	4-OCH3–pyridin-3-yl	3-Br–4-OH–Ph–	H	O	O	8.40
31	4-CH3–pyridin-3-yl	3-Br–4-OH–Ph–	H	O	O	7.17
32	4-F–pyridin-3-yl	3-Br–4-OH–Ph–	H	O	O	7.68
33	4-Cl–pyridin-3-yl	3-Br–4-OH–Ph–	H	O	O	7.70
34	4-N(CH3)2–pyridin-3-yl	3-Br–4-OH–Ph–	H	O	O	8.40
35	4-OCH3–Ph–	4-OH–Ph–	H	S	S	6.91
36	4-OCH3–Ph–	3-CH3–4-OH–Ph–	H	S	S	7.70
37	4-OCH3–Ph–	3-OCH3–4-OH–Ph–	H	S	S	6.60
38	4-OCH3–Ph–	3-F–4-OH–Ph–	H	S	S	8.70
39	4-OCH3–Ph–	3-Cl–4-OH–Ph–	H	S	S	8.40
40	4-OCH3–Ph–	2-Cl–4-OH–Ph–	H	S	S	8.30
41	4-OCH3–Ph–	3,5-Cl–4-OH–Ph–	H	S	S	7.92
42	4-OCH3–Ph–	3,5-F–4-OH–Ph–	H	S	S	8.30
43	4-OCH3–Ph–	3-Cl–4-OH–5-F–Ph–	H	S	S	9.00
44	4-OCH3–Ph–	4-OH–pyridin-2-yl	H	S	S	7.05
45	4-OCH3–Ph–	4-OH–3-Br–pyridin-2-yl	H	S	S	7.40
46	4-OCH3–Ph–	3-Br–4-OH–Ph–	CH3	S	S	7.05
47	4-OCH3–Ph–	3-Cl-5-F, 4-OH	CH	C	S	9.00
48	4-OCH3–Ph–	4-OH	N	C	S	7.05
49	4-OCH3–Ph–	3-Br, 4-OH	N	C	S	7.38

49 4-OCH3–Ph– 3-Br, 4-OH N C S 7.38

[a]Adapted from Harada et al. (2012).
[b]Me, methyl; Ph, phenyl; pIC_{50}, negative logarithm of the half-maximal inhibitory concentration.

2.3 Ligand Structure Preparation

The chemical structures of the 49 benzylidene-derived analogs were constructed using MolView, an open-source web-based molecular visualization platform. Canonical Simplified Molecular Input Line Entry System notations were generated for each analog and converted into structure-data files using Open Babel version 3.1.1, following the procedure described by O'Boyle et al. (2011). The resulting SDF files were used as input files for molecular descriptor computation. This preparation step ensured that all structures were represented in a compatible format for downstream QSAR analysis.

2.4 Molecular Descriptor Computation and Data Pretreatment

Molecular descriptors were computed using ChemDes, an integrated web-based platform for descriptor and fingerprint calculation described by Dong et al. (2015). Chemopy descriptors were selected because these include constitutional, topological, geometrical, electrostatic, and physicochemical descriptors that are useful in chemoinformatics and QSAR modeling. A total of 633 descriptors were initially calculated for each compound.

Before model generation, descriptor pretreatment was performed using Data Pretreatment GUI version 1.2 from the Drug Theoretics and Cheminformatics Laboratory. Constant and highly intercorrelated descriptors were removed using the

default variance cutoff of 0.001 and correlation coefficient cutoff of 0.99. This step was performed to reduce descriptor redundancy, minimize collinearity, and improve the interpretability and stability of the generated model.

2.5 Training and Test Set Division

The pretreated dataset was divided into training and test sets using Dataset Division GUI version 1.0. The Kennard-Stone permutation algorithm was applied to ensure rational and representative selection of compounds for model development and validation. Following an 80:20 division, 40 compounds were assigned to the training set and 9 compounds were assigned to the test set. The training set was used to generate the QSAR model, while the test set was used for external validation. To evaluate whether the training and test sets adequately represented the chemical space of the dataset, diversity validation was performed using normalized mean distance scores.

2.6 QSAR Model Generation

A genetic algorithm-based multilinear regression model was generated using DTC-QSAR version 1.0.5. Multilinear regression was used to establish a mathematical relationship between molecular descriptors as independent variables and pIC_{50} values as the dependent variable. The general QSAR equation is shown in Equation 2.

$$pA = C0 + C1d1 + C2d2 + C3d3 + \ldots + Cidi \quad (2)$$

where pA represents the biological activity expressed as a negative logarithm, C0, is the intercept, Ci represents the coefficient of each descriptor, and di represents the computed molecular descriptor.

Genetic algorithm-based descriptor selection was performed using 100 iterations, a mutation probability of 0.3, and a maximum of eight descriptors per equation. The best model was selected based on statistical performance, predictive ability, and mean absolute error-based criteria. The final model was interpreted based on the descriptors retained in the generated equation.

2.7 QSAR Model Validation and Predictive Reliability Assessment

2.7.1 Internal Validation

The generated QSAR model was first evaluated using internal validation metrics to determine goodness of fit, internal predictive ability, and robustness. The coefficient of determination, adjusted coefficient of determination, F-test, standard error of estimation, leave-one-out cross-validated coefficient, modified squared correlation coefficients, and mean absolute error criteria were calculated. The following internal validation thresholds were adopted from established QSAR validation guidelines: $R^2 > 0.6$, $Q^2LOO > 0.5$, $R^2 - Q^2LOO < 0.2$, scaled average $Rm^2LOO > 0.5$, scaled $\Delta Rm^2LOO < 0.2$, and a statistically significant F-value at $\alpha = 0.05$ (Golbraikh & Tropsha, 2002; Kiralj & Ferreira, 2009). The standard error of estimation was interpreted as acceptable when close to zero.

2.7.2 Robustness and Chance Correlation Assessment

Model robustness was assessed using leave-N-out cross-validation, with N values ranging from 1 to 7. The resulting Q^2LNO values were compared with Q^2LOO, with minimal deviation indicating a robust model. To determine whether model performance resulted from chance correlation, y-randomization was performed using 50 randomly generated models, following recommended QSAR validation procedures (Eriksson et al., 2003; Kiralj & Ferreira, 2009). The y-randomization intercept values were considered acceptable if the R^2 intercept was less than 0.3 and the Q^2LNO intercept was less than 0.05.

2.7.3 External Validation

External validation was performed using the independent test set consisting of 9 compounds. Predictive performance was evaluated using the coefficient of determination for prediction, root mean square error of prediction, modified squared correlation coefficients, and Golbraikh-Tropsha criteria. The model was considered externally predictive if $R^2PRED > 0.5$, $R^20 > 0.5$, scaled average $Rm^2 > 0.5$, and scaled $\Delta Rm^2 < 0.2$. The Golbraikh-Tropsha criteria were also applied to further assess external predictivity. The accepted thresholds were as follows: $| R20 - R'20 | < 0.3$; $0.85 < k < 1.15$; $0.85 < k' < 1.15$; $(r2 - r02)/r2 < 0.1$; and $(r2 - r'02)/r2 < 0.1$ (Golbraikh & Tropsha, 2002). These parameters were used to determine whether the predicted and observed activities of the test compounds showed acceptable agreement.

2.7.4 Applicability Domain Analysis

Applicability domain analysis was performed to define the chemical space in which the QSAR model could generate reliable predictions. For the training and test sets, applicability domain was assessed using Euclidean distance-based analysis. Compounds outside the defined domain were considered potential structural or response outliers.

2.7.5 True External Prediction

A true external prediction set was prepared to evaluate the model's ability to estimate the activity of new query compounds with no experimental pIC_{50} values. Structurally similar compounds were identified from the ZINC database using a 2D

similarity search approach. After removing duplicates, eight structurally related compounds were selected for prediction. The selected true external compounds are shown in Figure 2.

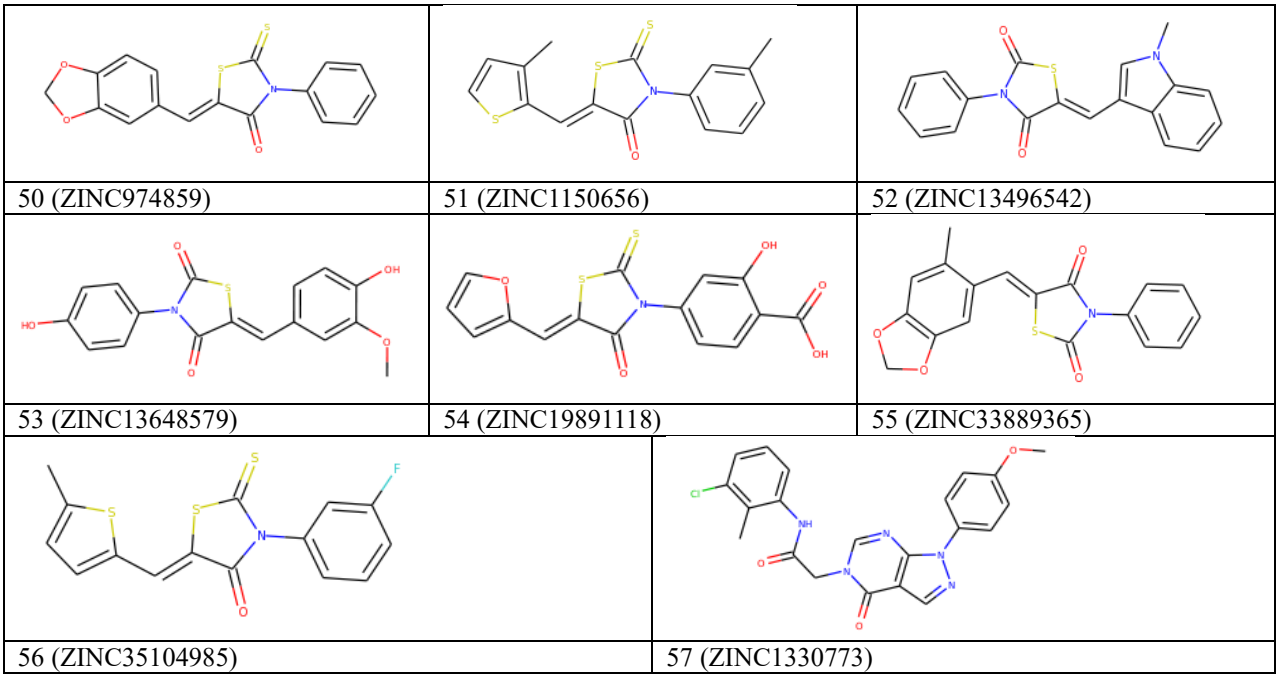

Fig. 2. True external set compounds selected from the ZINC database.

The selected compounds were structurally similar to the benzylidene-derived analogs in the modeling dataset and were used to evaluate the predictive reliability of the generated QSAR model.

The molecular descriptors included in the final QSAR model were computed for the true external compounds. Predicted pIC_{50} values and prediction reliability were determined using Prediction Reliability Indicator version 1.0, as described by Roy et al. (2018). Predictions were classified as good, moderate, or poor based on the software's weighting scheme. The applicability domain of the true external compounds was assessed using the model disturbance index.

2.8 Homology Model Construction for Molecular Docking

Because no experimentally resolved crystallographic structure of human 17β-hydroxysteroid dehydrogenase type 3 was available for docking, a homology modeling approach was used. The receptor model was reconstructed using Swiss-Model, following the approach described in previous structure-based studies involving 17β-hydroxysteroid dehydrogenase type 3 (Vicker et al., 2009; Engeli et al., 2017). The template used was the orthorhombic crystal structure of bulky-bulky ketone-specific alcohol dehydrogenase from Comamonas testosteroni with Protein Data Bank template 6ze0.1. This template was selected because of its structural and functional similarity to the target enzyme and its reported use in related modeling studies. The reconstructed homology model was checked for relevant active site residues, including serine and tyrosine residues reported in the literature. The model was then prepared for docking using AutoDockTools version 1.5.6.

2.9 Molecular Docking Protocol

Molecular docking was performed using AutoDockTools version 1.5.6 to estimate ligand binding affinity and identify possible receptor-ligand interactions (Morris et al., 2009). The receptor and ligand structures were prepared before docking. Water molecules were removed from the receptor structure to reduce ambiguity in ligand binding interactions. Polar hydrogen atoms were added, and Kollman charges were assigned to the receptor and ligands. Prepared receptor and ligand files were saved in PDBQT format.

The AutoGrid procedure was used to define the docking search space. A three-dimensional grid box was centered on the active site of the homology model using the following coordinates: x = -6.583, y = -8.666, and z = -5.528, with a grid spacing of 0.375 Å. For each ligand, 100 docking simulations were performed. The Lamarckian Genetic Algorithm was used to identify the lowest energy-binding conformations. Docked poses were ranked based on estimated free binding energy, and the ligand with the most favorable docking score was selected for detailed post-docking analysis. Post-docking interactions were visualized using AutoDockTools and Protein-Ligand Interaction Profiler (Morris et al., 2009; Salentin et al., 2015). Hydrogen bonds, hydrophobic interactions, van der Waals interactions, and active site-adjacent contacts were examined to support the mechanistic interpretation of the QSAR descriptors.

2.10 Mechanistic Interpretation of the QSAR Model

The final QSAR model was interpreted by examining the physicochemical meaning of the retained molecular descriptors and correlating these descriptors with docking-based ligand-receptor interactions. Descriptor contributions were classified as positive or negative based on their coefficients in the final model. Positive coefficients indicated that increasing descriptor values were associated with increased predicted inhibitory activity, while negative coefficients indicated that increasing descriptor values were associated with decreased predicted inhibitory activity.

Mechanistic interpretation focused on descriptors associated with atomic polarizability, hydrophobicity, electrospatial topology, electrotopological state indices, and molecular autocorrelation. The docking results were used to support the descriptor-based interpretation by identifying whether the most active analogs interacted with hydrophobic regions, polar residues, or active site-adjacent amino acids of the receptor model.

RESULTS AND DISCUSSION

3.1 Generated GA-MLR QSAR Model

A genetic algorithm-based multilinear regression model was generated using the pretreated molecular descriptor matrix of the 49 benzylidene-derived analogs. The final model contained eight descriptors and was developed using 40 training set compounds, while 9 compounds were reserved for external validation. The generated model is shown in Equation 3.

pIC50 = 7.6536 + 3.0253 (GATSe3) + 0.0653 (LogP2) - 0.0173 (EstateVSA5) + 2.7153 (MATSp7) + 4.386 (bcutp6) + 1.6452 (MATSm8) - 5.0072 (bcutp5) - 1.3061 (GATSe8) (3)

The descriptors retained in the model included GATSe3, LogP2, EstateVSA5, MATSp7, bcutp6, MATSm8, bcutp5, and GATSe8 (Table 2). Among these, GATSe3, LogP2, MATSp7, bcutp6, and MATSm8 contributed positively to predicted inhibitory activity, while EstateVSA5, bcutp5, and GATSe8 contributed negatively. This indicates that increases in the positively contributing descriptors were associated with higher predicted pIC_{50} values, while increases in the negatively contributing descriptors were associated with lower predicted pIC_{50} values.

Table 2. Molecular descriptors included in the final GA-MLR QSAR model.

Descriptor	Description	Contribution
GATSe3	Geary Autocorrelation-Lag3/Weighted by ASE	Positive
LogP2	Square of LogP Value Based on the Ghost-Crippen Method	Positive
EstateVSA5	MOE-Type/Estate Indices and Surface Area Contributions	Negative
MATSp7	Moran Autocorrelation-Lag7/Weighted by AP	Positive
bcutp6	Highest Eigenvalue.6 of Burden Matrix/Weighted by AP	Positive
MATSm8	Moran Autocorrelation-Lag8/Weighted by AM	Positive
bcutp5	Highest Eigenvalue.5 of Burden Matrix/Weighted by AP	Negative
GATSe8	Geary Autocorrelation-Lag8/Weighted by ASE	Negative

The inclusion of autocorrelation, hydrophobicity, electrotopological, and Burden matrix descriptors suggests that the inhibitory activity of benzylidene-derived analogs is influenced by molecular topology, electrostatic distribution, hydrophobicity, atomic polarizability, and mass-related structural features. Molecular descriptors are useful in QSAR modeling because they convert structural and physicochemical properties into numerical variables that can be correlated with biological activity (Puzyn et al., 2010; Todeschini & Consonni, 2008). These descriptor classes are also consistent with the principle that ligand-enzyme binding is influenced not only by the presence of specific substituents, but also by their topological placement and physicochemical environment (Tropsha, 2010).

3.2 Diversity Validation and Applicability of the Training and Test Sets

The training and test sets were evaluated using normalized mean distance scores to determine whether the selected compounds adequately represented the chemical space of the dataset. The diversity validation plots showed that the training and test compounds were distributed across a range of pIC_{50} values and normalized mean distances (Figure 3). No structural outliers were detected, and all analogs were located within the model applicability domain.

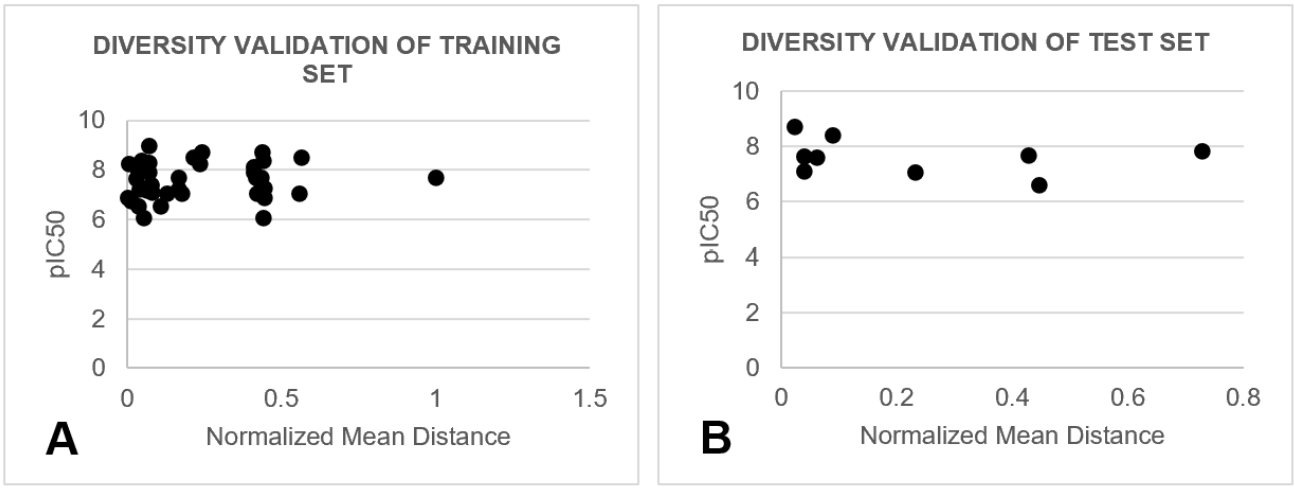

Fig. 3. Diversity validation plots of the training and test sets. Normalized mean distance scores were plotted against observed pIC_{50} values to assess chemical diversity. The distribution of compounds suggests that the training and test sets were structurally representative of the benzylidene-derived analog dataset.

This result supports the rationality of the Kennard-Stone-based dataset division. A structurally representative training set is essential in QSAR modeling because the model can only generate reliable predictions within the chemical space represented during model development (Eriksson, 2003; Tropsha, 2010). Likewise, a sufficiently diverse test set improves the value of external validation by allowing the model to be assessed on compounds that are related to, but independent from, the training set (Koutsoukas et al., 2014).

3.3 Internal Validation of the QSAR Model

The generated model showed strong internal validation performance (Table 3). The coefficient of determination was R^2 = 0.8994, indicating that the model explained approximately 89.94% of the variance in the training set pIC_{50} values. The leave-one-out cross-validated coefficient was Q^2LOO = 0.8366, suggesting good internal predictive ability. The difference between R^2 and Q^2LOO was 0.0628, which was below the accepted threshold of 0.2 and therefore suggested that the model was not overfitted.

Table 3. Internal validation parameters of the final GA-MLR QSAR model.

Parameter a	Value	Martins & Melo (2019)	Acceptable Criteria
R2	0.8994	0.77	> 0.6; Passed
R2Adjusted	0.8734	–	> 0.6; Passed
F-Value	2.31x10-13	–	< 0.01; Significant
SEE	0.2601	0.44	Passed
Q2LOO	0.8366	0.61	> 0.5; Passed
R2 – Q2LOO	0.0628	0.16	< 0.2; Passed
Scaled Average Rm2LOO	0.7735	0.50	> 0.5; Passed
Scaled Δ Rm2LOO	0.0623	0.14	< 0.2; Passed
MAE (100% Data)	0.2279	–	Passed
MAE Error (95% Data)	0.2002	–	Passed
Prediction Quality	0.718	–	Moderate

[a]R^2, coefficient of determination; SEE, standard error of estimation; Q^2LOO, leave-one-out cross-validated coefficient; MAE, mean absolute error; Rm^2LOO, modified squared correlation coefficient.

The internal validation results indicate that the model had good explanatory power and acceptable internal predictivity. In QSAR studies, R^2 reflects goodness of fit, while Q^2LOO provides an estimate of internal predictive performance through cross-validation (Golbraikh & Tropsha, 2002; Kiralj & Ferreira, 2009). The low standard error of estimation and significant F-value further support the statistical adequacy of the regression model. The high Q^2LOO value is particularly important because QSAR models may show strong fitting performance but poor predictive performance when overfitted (Tropsha, 2010). In this model, the small difference between R^2 and Q^2LOO supports the stability of the descriptor combination.

Compared with the previously published QSAR model of Martins and Melo (2019), the present model showed higher R^2 and Q^2LOO values. However, this comparison should be interpreted cautiously because differences in modeling method, descriptor selection, dataset processing, and validation approach may influence model performance. The stronger internal statistics suggest that the present GA-MLR model provides an improved computational fit for the selected benzylidene-derived analog dataset, but it does not replace the need for experimental validation.

3.4 Predicted Vs. Observed Activity and Residual Analysis

The response plot of predicted versus observed pIC_{50} values showed close agreement between the experimental and predicted activities of the training and test compounds (Figure 4). This finding supports the goodness of fit and predictive performance of the generated GA-MLR model.

Fig. 4. Response plot of predicted versus observed pIC_{50} values for the training and test sets. Predicted pIC_{50} values were plotted against observed pIC_{50} values to evaluate agreement between experimental and model-predicted inhibitory activities.

The standardized residual plot showed that residual values were generally within ±2 units, indicating acceptable error distribution (Figure 5). Test set compounds showed greater scatter than training compounds, which may reflect greater structural diversity among the compounds reserved for external validation.

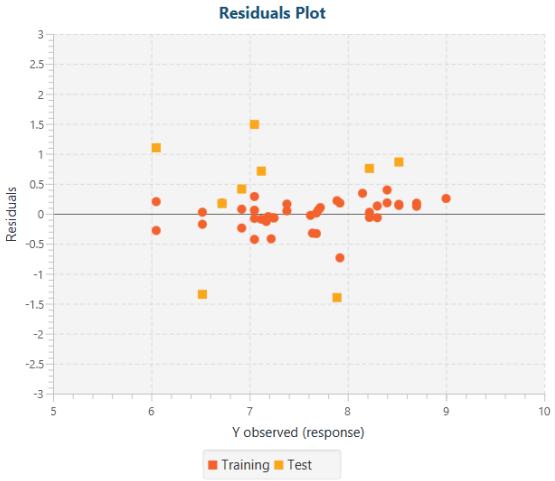

Fig. 5. Standardized residual plot of the GA-MLR QSAR model. Standardized residual values were plotted against observed pIC_{50} values to evaluate prediction error distribution. Residuals were generally within ±2 units, indicating acceptable agreement between predicted and observed inhibitory activities.

Residual analysis is important because a model with high R^2 may still show systematic prediction errors. In regression-based QSAR modeling, residual plots are used to assess whether prediction errors are randomly distributed and whether individual compounds exert disproportionate influence on the model (Kiralj & Ferreira, 2009). In this study, the absence of extreme residuals suggests that no individual compound exerted a disproportionate influence on the model. The observed scatter among test compounds is expected in external validation, particularly when the test set contains compounds with broader structural variation. Overall, the response and residual plots support the statistical validation results and suggest acceptable model stability.

3.5 Robustness and Chance Correlation Assessment

The leave-N-out cross-validation showed that the average Q^2LNO value was 0.8320, which was close to the Q^2LOO value of 0.8366 (Figure 6A). The difference between these values was small, indicating that the model retained predictive stability even when multiple compounds were removed during validation. The largest deviation was observed at Q^2L7O, but the value remained within an acceptable range.

The y-randomization test showed that randomly generated models had substantially lower R^2 and Q^2 values than the original model (Figure 6B). The intercept values were within accepted limits, supporting the conclusion that the final model was not generated by chance correlation.

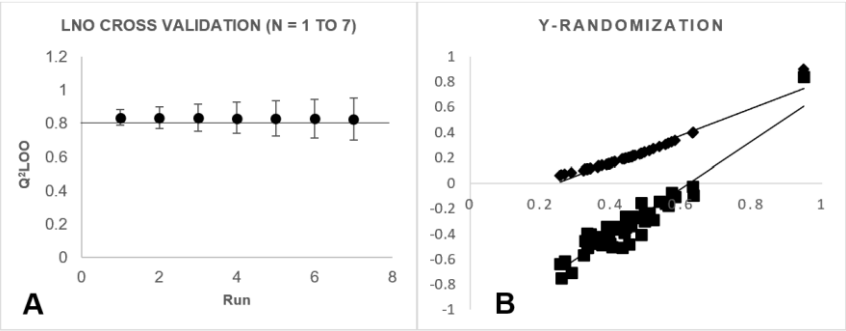

Fig. 6. Robustness and chance correlation assessment of the GA-MLR QSAR model. (A) Leave-N-out cross-validation plot showing Q²LNO values from N = 1 to 7. (B) Y-randomization plot comparing the original model with randomly generated models. Lower validation performance among randomized models supports the absence of chance correlation.

These findings strengthen the reliability of the model. In QSAR modeling, chance correlation is a common concern, especially when descriptor selection is performed from a large descriptor pool. Y-randomization is commonly recommended to determine whether the relationship between descriptors and biological activity is statistically meaningful rather than random (Eriksson et al., 2003; Kiralj & Ferreira, 2009). Likewise, leave-N-out validation evaluates whether the model remains stable after systematic removal of subsets of compounds (Kiralj & Ferreira, 2009). Together, these findings support the robustness of the generated GA-MLR model.

3.6 External Validation of Predictive Performance

External validation was performed using the 9-compound test set. The model showed good external predictive performance, with R^2PRED = 0.8792 and RMSEP = 1.1709 (Table 4). The model also satisfied the modified Rm^2 criteria and Golbraikh-Tropsha validation parameters. The values of k and k′ were within the accepted range of 0.85 to 1.15, and both and $(r^2 - r_0'^2)/r^2$ were below 0.1.

Table 4. External validation parameters of the final GA-MLR QSAR model.

Parameter	Value	Martins & Melo (2019)	Acceptable Criteria
R2PRED	0.8792	0.74	> 0.5 Passed
R20	0.8540	–	> 0.5; Passed
RMSEP	1.1709	0.35	Passed
Scaled Average Rm2 (Test)	0.7661	0.61	> 0.5; Passed
Scaled ∆ Rm2 (Test)	0.0295	0.20	< 0.2; Passed
| R20 – R'20 |	0.08587	0.13	< 0.3; Passed
k	1.03364	1.00	0.85 < k < 1.15; Passed
k'	0.95155	0.10	0.85 < k' < 1.15; Passed
(r2 – r02)/r2	0.0286	–	< 0.1; Passed
(r2 – r'02)/r2	0.076	–	< 0.1; Passed

The external validation findings indicate that the model can predict the inhibitory activity of compounds not used during model generation. External validation is considered essential in QSAR modeling because a model's practical value depends on its ability to predict new compounds rather than merely fit the training set (Golbraikh & Tropsha, 2002; Tropsha, 2010). The modified Rm^2 metrics further assess agreement between observed and predicted activities and help address limitations of using correlation-based parameters alone (Ojha et al., 2011). Although RMSEP was higher than that reported in the comparison model, the other external validation parameters met accepted criteria, suggesting that the model retained useful predictive ability.

3.7 Prediction Quality of Test Set Compounds

The predicted pIC_{50} values of the test set compounds were compared with their observed pIC_{50} values (Table 5). Most compounds showed moderate prediction quality, while one compound showed good prediction quality. Residuals ranged from -1.40 to 1.49, and all test set analogs were within the applicability domain of the model.

Table 5. Observed and predicted pIC_{50} values of test set compounds.

No.	Observed pIC50	Predicted pIC50	Residuals a	Prediction Quality

1	7.85	6.75	1.1	Moderate
25	7.60	7.19	0.41	Moderate
28	7.05	8.39	-1.34	Moderate
30	7.13	6.96	0.17	Good
31	7.66	6.80	0.86	Moderate
35	7.70	6.80	0.90	Moderate
36	8.40	6.91	1.49	Moderate
41	6.57	7.97	-1.40	Moderate
42	8.70	7.94	0.76	Moderate

[a]Residual = observed pIC_{50} - predicted pIC_{50}.

The moderate prediction quality for most test compounds suggests that the model is useful for prioritization rather than definitive activity prediction. This distinction is important for in silico drug discovery because computational models are intended to reduce screening burden and guide compound prioritization, but predicted values should still be confirmed through experimental assays (Tropsha, 2010; Nantasenamat, 2020). The presence of residual variation also indicates that additional structural or physicochemical features not captured by the eight selected descriptors may contribute to 17β-HSD3 inhibition.

3.8 True External Prediction and Applicability Domain

A true external set of eight structurally related compounds from the ZINC database was evaluated using the final QSAR model. The predicted pIC_{50} values ranged from 7.21 to 9.98 (Table 6). Seven of the eight compounds showed good prediction quality, while one compound showed moderate prediction quality. Applicability domain analysis using the model disturbance index showed that all true external compounds except Compound 51 were within the model domain (Figure 7).

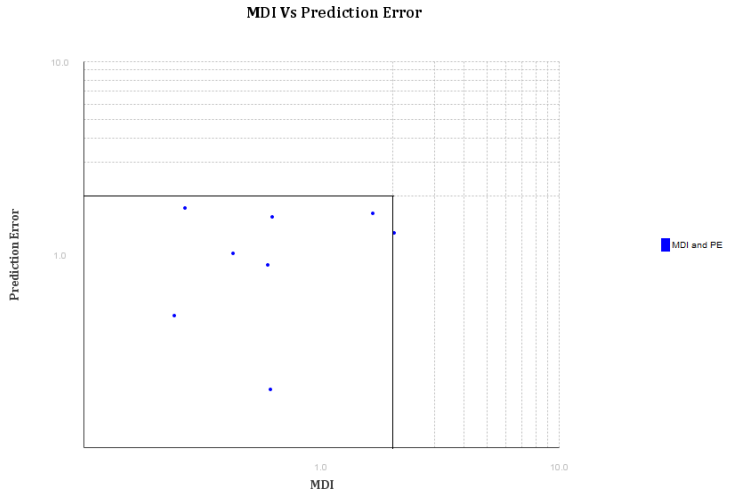

Fig. 7. Applicability domain analysis of the true external validation set. The applicability domain of the true external compounds was assessed using the model disturbance index. Compounds within the applicability domain were considered to have more reliable predictions, while compounds outside the domain were considered less reliable.

Table 6. Prediction reliability of true external set compounds.

No.	Molecular Descriptors								Predict pIC50	Quality
	GATSe3	LogP2	EstateVSA5	MATSp7	bcutp6	MATSm8	bcutp5	GATSe8		
50	1.011	14.601	4.9	0.064	2.7	0.066	2.83	0.899	8.36	Good
51	1.287	22.76	16.237	-0.113	2.787	-0.012	2.909	0.077	9.98	Moderate
52	1.14	19.529	18.209	0.032	2.7	0.019	2.933	1.29	7.65	Good
53	1.033	11.204	18.209	-0.034	2.662	0.071	2.824	0.805	7.70	Good
54	1.039	9.543	18.209	-0.008	2.687	0.225	2.91	1.118	7.21	Good
55	1.027	15.718	30.341	-0.063	2.661	0.082	2.879	0.733	7.52	Good
56	1.04	21.173	23.47	-0.008	2.672	-0.151	2.716	0.641	8.79	Good
57	0.962	19.091	18.33	-0.288	2.92	-0.096	2.989	0.74	7.43	Good

The true external prediction results suggest that the model may be useful for screening structurally related benzylidene-derived compounds. However, the prediction for Compound 51 should be interpreted cautiously because it was outside the

applicability domain. Applicability domain assessment is an important step in QSAR validation because prediction reliability depends on whether a query compound falls within the chemical and descriptor space represented by the model (Eriksson et al., 2003; Yan et al., 2014). A compound outside the applicability domain may be structurally or physicochemically different from the training set compounds, making its predicted activity less reliable even if the predicted pIC_{50} value appears favorable. The use of prediction reliability indicators for new query chemicals further supports more cautious interpretation of QSAR-derived predictions (Roy et al., 2018).

3.9 Molecular Docking and Descriptor-Based Mechanistic Interpretation

Molecular docking was performed to support the mechanistic interpretation of the retained QSAR descriptors. The docking model showed that the selected ligand was stabilized by interactions within the active site and active site-adjacent regions of the receptor model (Figure 8). Hydrophobic residues were observed around the central and peripheral regions of the ligand-binding space, while polar residues such as serine, tyrosine, and asparagine were positioned near electron-rich ligand regions.

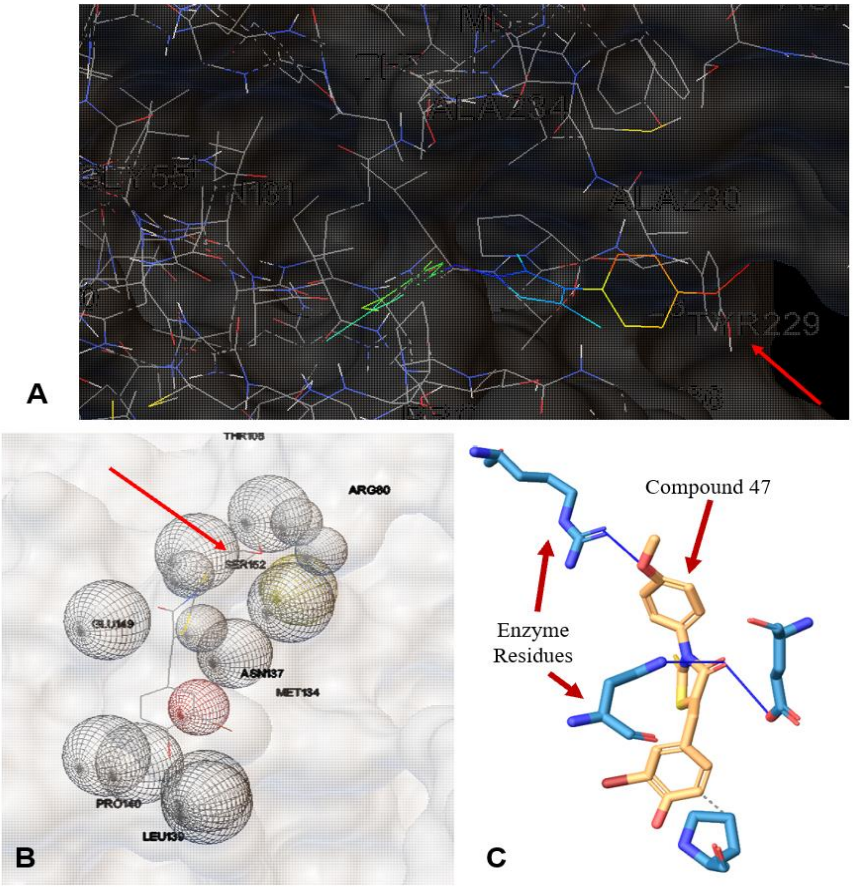

Fig. 8. Molecular docking model of the 3D space surrounding the 17β-hydroxysteroid dehydrogenase type 3 active site using the most active compound. (A) Docking model showing the ligand within the receptor binding region. (B) Electron-rich ligand regions positioned near polar active site residues. (C) Two-dimensional interaction diagram showing hydrogen bonds and van der Waals interactions. Hydrogen bonds and noncovalent interactions contributed to stabilization of the ligand-receptor complex.

The descriptor-based interpretation suggests that 17β-HSD3 inhibition among the benzylidene-derived analogs is influenced by electrospatial topology, hydrophobicity, and atomic polarizability. GATSe3 and GATSe8 are Geary autocorrelation descriptors weighted by atomic Sanderson electronegativity. Autocorrelation descriptors describe how molecular properties are distributed across specific topological distances within a molecule (Todeschini & Consonni, 2008; Puzyn et al., 2010). Their opposite contributions indicate that the placement of electronegative atoms at different topological distances may influence inhibitory activity in different directions. Specifically, electronegative features at shorter topological distances may favor activity, while similar features at longer topological distances may reduce predicted activity.

MATSp7 and MATSm8 are Moran autocorrelation descriptors weighted by atomic polarizability and atomic mass, respectively. Their positive coefficients suggest that polarizable atoms and mass-related structural features at specific topological lags may support stronger inhibitory activity. This is consistent with the docking-based observation that ligand

stabilization may involve noncovalent interactions within the binding pocket. Similar interpretations of autocorrelation descriptors have been used in QSAR studies to connect spatial distributions of molecular properties with biological activity (Singh et al., 2009; Todeschini & Consonni, 2008).

LogP2 contributed positively to inhibitory activity, suggesting that hydrophobicity is favorable for the benzylidene-derived analogs. LogP is a widely used molecular descriptor that estimates hydrophobicity and is relevant to ligand binding, membrane permeability, and drug-likeness (Kujawski et al., 2012). This result may reflect the importance of hydrophobic stabilization within the ligand-binding region. Since 17β-HSD3 is associated with microsomal localization, hydrophobic features may also influence membrane-associated access and ligand orientation, although this inference requires experimental confirmation (George et al., 2010).

EstateVSA5 contributed negatively to predicted activity, indicating that certain electrotopological surface area features may reduce inhibitory activity when increased. E-state descriptors encode information on the electronic and topological environment of atoms and have been used in QSAR modeling to relate atom-level electronic states to biological activity (Abou-Shaaban et al., 1996; Roy & Mitra, 2012). This suggests that not all electron-rich or polar surface contributions are favorable; their effect likely depends on the location, orientation, and interaction compatibility of substituents within the binding site.

The BCUT descriptors bcutp6 and bcutp5 also showed opposite contributions. BCUT descriptors are derived from modified connectivity matrices and encode molecular properties such as atomic charge, polarizability, and hydrogen-bonding capacity (Pearlman & Smith, 1998; Antanasijevic et al., 2016). Since these descriptors are related to atomic polarizability and molecular connectivity, their directional effects suggest that polarizability contributes to activity in a topology-dependent manner. Increasing bcutp6 may improve activity, whereas increasing bcutp5 may reduce activity. This indicates that the overall distribution of polarizable features, rather than polarizability alone, may influence 17β-HSD3 inhibition.

Overall, the docking-supported mechanistic interpretation indicates that the inhibitory activity of the benzylidene-derived analogs is not governed by a single structural property. Instead, activity appears to depend on the coordinated influence of hydrophobicity, electronegativity distribution, atomic polarizability, and topological arrangement. These findings are consistent with the general view that reliable QSAR interpretation should integrate statistical validation with chemically meaningful descriptor analysis and, when appropriate, structure-based modeling (Tropsha, 2010; Nantasenamat, 2020). Therefore, the generated model may be useful as a computational tool for prioritizing structurally related compounds for further experimental evaluation.

CONCLUSION

This study developed and validated an in silico 2D-QSAR model for predicting the inhibitory activity of benzylidene-derived analogs against 17β-hydroxysteroid dehydrogenase type 3. The final GA-MLR model incorporated eight molecular descriptors and demonstrated good internal and external validation performance, with acceptable goodness of fit, predictive ability, robustness, and low probability of chance correlation. Applicability domain analysis further supported the reliability of the model for compounds structurally related to the training dataset. Descriptor-based interpretation, supported by molecular docking, suggested that inhibitory activity is influenced by hydrophobicity, atomic polarizability, electronegativity distribution, and electrospatial topology. These findings indicate that both physicochemical properties and the topological placement of molecular features may contribute to ligand interaction with the 17β-hydroxysteroid dehydrogenase type 3 binding region.

Overall, the validated model may serve as a useful computational tool for virtual screening and rational design of structurally related benzylidene-derived analogs as potential 17β-hydroxysteroid dehydrogenase type 3 inhibitors. However, because the findings are based on computational modeling, further in vitro and in vivo studies are needed to confirm the predicted inhibitory activity, selectivity, pharmacokinetic behavior, toxicity profile, and therapeutic relevance of candidate compounds. Future studies may also compare the present GA-MLR approach with other modeling methods, such as partial least squares regression, support vector regression, random forest, or other machine learning-based algorithms, using larger and more structurally diverse datasets. Improved human-derived homology models or experimentally resolved human 17β-hydroxysteroid dehydrogenase type 3 structures, once available, may also strengthen docking-based interpretation and biological applicability.

AcknowledgEments

The researchers wish to thank Dr. Kunal Roy for the support on statistical analysis and software use.

Competing interests

Authors have declared that no competing interests exist.

Consent
Not applicable because this study did not involve human participants.

Ethical approval
Not applicable because this study used previously published chemical and biological activity data and did not involve human participants, animal subjects, or patient records.

REFERENCES

1. Abou-Shaaban, R., Al-Khamees, H., Abou-Auda, H., & Simonelli, A. (1996). Atom Level Electrotopological State Indexes in QSAR: Designing and Testing Antithyroid Agents. Pharmaceutical Research, 13, 129-136. https://doi.org/10.1023/A:1016049921842
2. Antanasijevic, J., Antanasijevic, D., Pocajt, V., Trisovic, N., & Fodor-Csorba, K. (2016). A QSPR study on the liquid crystallinity of five-ring bent-core molecules using decision trees, MARS and artificial neural networks. Royal Society of Chemistry Advances, 6, 18452-18464. https://doi.org/10.1039/C5RA20775D
3. Cheng, Y., Yang, Y., Wu, Y., Wang, W., Xiao, L., Zhang, Y., Tang, J., Huang, Y., Zhang, S., Xiang, Q. (2020). The Curcumin Derivative, H10, Suppresses Hormone-Dependent Prostate Cancer by Inhibiting 17B-Hydroxysteroid Dehydrogenase Type 3. Frontiers in Pharmacology, 11(637). https://doi.org/10.3389/fphar.2020.00637
4. Dong, J., Cao, D., Miao, H., Liu, S., Deng, B., Yun, Y., Wang, N., Lu, A., Zeng, W., Chen, A.F. (2015). ChemDes: an integrated web-based platform for molecular descriptor and fingerprint computation. Journal of Cheminformatics, 7(60), PMCID: PMC4674923. https://doi.org/10.1186/s13321-015-0109-z
5. Engeli, R., Tsachaki, M., Hassan, H., Sager, C., Essawi, M., Gad, Y., Kamel, A., Mazen, I., Odermatt, A. (2017). Biochemical Analysis of Four Missense Mutations in the HSD17B3 Gene Associated With 46,XY Disorders of Sex Development in Egyptian Patients. Journal of Sexual Medicine, 14(9), 1165-1174. https://doi.org/10.1016/j.jsxm.2017.07.006
6. Eriksson, L., Jaworska, J., Worth, A., Cronin, M., McDowell, R., & Gramatica, P. (2003). Methods for Reliability and Uncertainty Assessment and for Applicability Evaluations of Classification- and Regression-Based QSARs. Environmental Health Perspectives, 111(10), 1361-1375. https://doi.org/10.1289/ehp.5758
7. George, M., New, M., Ten, S., Sultan, C., & Bhangoo, A. (2010). The Clinical and Molecular Heterogeneity of 17B-HSD-3 Enzyme Deficiency. Hormone Research in Pediatrics, 74, 229-240. https://doi.org/10.1159/000318004
8. Golbraikh, A., & Tropsha, A. (2002). Beware of q2! Journal of Molecular Graphics & Modelling, 20(4), 269-276. https://doi.10.1016/s1093-3263(01)00123-1.
9. Harada, K., Kubo, H., Abe, J., Haneta, M., Conception, A., Inoue, S., Okada, S., Nishioka, K. (2012). Discovery of potent and orally bioavailable 17b-hydroxysteroid dehydrogenase type 3 inhibitors. Bioorganic and Medicinal Chemistry, 20, 3242-3254. https://doi.org/10.1016/j.bmc.2012.03.052
10. Kiralj, R., & Ferreira, M. (2009). Basic validation procedures for regression models in QSAR and QSPR studies: Theory and application. Journal of the Brazilian Chemical Society, 20(4), 770-787. https://doi.10.1590/S0103-50532009000400021
11. Koutsoukas, A., Paricharak, S., Galloway, W., Spring, D., Jzerman, A., Glen, R., Marcus, D., Bender, A. (2014). How Diverse Are Diversity Assessment Methods? A Comparative Analysis and Benchmarking of Molecular Descriptor Space. Journal of Chemical Information and Modeling, 54(1), 230-242. https://doi.org/10.1021/ci400469u
12. Kujawski, J., Popielarska, H., Myka, A., Drabińska, B., & Bernard, M. (2012). The log P Parameter as a Molecular Descriptor in the Computer-aided Drug Design – an Overview. Computational Methods in Science and Technology, 18(2), 81-88. https://doi.org/10.12921/cmst.2012.18.02.81-88
13. Litwin, M., & Tan, H. (2017). The Diagnosis and Treatment of Prostate Cancer A Review. Clinical Review & Education, 317(24), 2532-2542. https://doi.org/10.1001/jama.2017.7248
14. Martins, J. P., & Melo, E. B. (2019). 4D-QSAR Study of 17β-Hydroxysteroid Dehydrogenase Type 3 Inhibitors. Journal of Brazilian Chemistry Society, 30(7), 1548-1557. https://doi.org/10.21577/0103-5053.20190052
15. Michaelson, M., Cotter, S., Gargollo, P., Zietman, A., Dahl, D., & Smith, M. (2008). Management of Complications of Prostate Cancer Treatment. A Cancer Journal for Clinicians, 58, 196-213. https://doi.org/10.3322/CA.2008.0002
16. Morris, G., Huey, R., Lindstrom, W., Sanner, M., Belew, R., Goodsell, D., & Olson, A. (2009). Autodock4 and AutoDockTools4: automated docking with selective receptor flexibility. J. Computational Chemistry, 16, 2785-2791. https://doi.org/10.1002/jcc.21256
17. Nantasenamat, C. (2020). Best Practices for Constructing Reproducible QSAR Models. Ecotoxicological QSARs, 55-75. https://doi.org/10.1007/978-1-0716-0150-1_3
18. Ning, X., Yang, Y., Deng, H., Zhang, Q., Huang, Y., Su, Z., Fu, Y., Xiang, Q., Zhang, S. (2017). Development of 17β-hydroxysteroid dehydrogenase type 3 as a target in hormone-dependent prostate cancer therapy. Steroids, 121, 10-16. https://doi.org/10.1016/j.steroids.2017.02.003

19. O'Boyle, N., Banck, M., James, C., Morley, C., Vandermeersch, T., & Hutchison, G. (2011). Open Babel: An open chemical toolbox. Journal of Cheminformatics, 3(33). https://doi.org/10.1186/1758-2946-3-33
20. Ojha, P., Mitra, I., Das, R., & Roy, K. (2011). Further exploring rm2 metrics for validation of QSPR models. Chemometrics and Intelligent Laboratory Systems, 107(1), 194-205. https://doi.org/10.1016/j.chemolab.2011.03.011
21. Pearlman, R., & Smith, K. (1998). Novel Software Tools for Chemical Diversity. Perspectives in Drug Discovery and Design, 9, 339-353. https://doi.org/10.1023/A:1027232610247
22. Puzyn, T., Leszczynski, J., & Cronin, M. (2010). Recent Advances in QSAR Studies Methods and Applications (Vol. 8). New York: Springer Science.
23. Rawla, P. (2019). Epidemiology of Prostate Cancer. World Journal of Oncology, 10(2), 63-89. https://doi.org/10.14740/wjon1191
24. Roy, K., & Mitra, I. (2012). Electrotopological state atom (E-state) index in drug design, QSAR, property prediction and toxicity assessment. Current Computer-Aided Drug Design, 8(2), 135-158. https://doi.org/10.2174/157340912800492366
25. Roy, K., Ambure, P., & Kar, S. (2018). How Precise Are Our Quantitative Structure−Activity Relationship Derived Predictions for New Query Chemicals? ACS Omega, 3, 11392-11406. https://doi.org/10.1021/acsomega.8b01647
26. Salentin, S., Schreiber, S., Haupt, V., Adasme, M., & Schroeder, M. (2015). PLIP: fully automated protein–ligand interaction profiler. Nucleic Acids Research, 43(W1), W443-W447. https://doi.org/10.1093/nar/gkv315
27. Singh, P., Kumar, R., Sharma, B., & Prabhakar, Y. (2009). Topological descriptors in modeling malonyl coenzyme A decarboxylase inhibitory activity: N-Alkyl-N-(1,1,1,3,3,3-hexafluoro-2-hydroxypropylphenyl)amide derivatives. Journal of Enzyme Inhibition and Medicinal Chemistry, 24(1), 77-85. https://doi.org/10.1080/14756360801915336
28. Spires, T., Fink, B., Kick, E., You, D., Rizzo, C., Takenaka, I., Lawrence, M., Ruan, Z., Salvati, M., Vite, G., Weinmann, R., Attar, R., Gottardis, M., Lorenzi, M. (2005). Identification of Novel Functional Inhibitors of 17B-Hydroxysteroid Dehydrogenase Type III (17B-HSD3). The Prostate, 65, 159-170. https://doi.org/10.1002/pros.20279
29. Todeschini, R., & Consonni, V. (2008). Handbook of Molecular Descriptors. John Wiley & Sons. https://doi.org/10.1002/9783527613106
30. Tropsha, A. (2010). Best practices for QSAR model development, validation, and exploitation. Molecular Informatics, 29(6-7), 476-488. https://doi.org/10.1002/minf.201000061
31. Vicker, N., Sharland, C., Heaton, W., Gonzalez, A., Bailey, H., Smith, A., Springall, J., Day, J., Tutill, H., Reed, M., Purohit, A., Potter, B. (2009). The Design of Novel 17β-Hydroxysteroid Dehydrogenase Type 3 Inhibitors. Molecular and Cellular Endocrinology, 301(1-2), 259-284. https://doi.org/10.1016/j.mce.2008.08.005
32. Yan, J., Zhu, W., Kong, B., Lu, H., Yun, Y., Huang, J., & Liang, Y. (2014). A Combinational Strategy of Model Disturbance and Outlier Comparison to Define Applicability Domain in Quantitative Structural Activity Relationship. Molecular Informatics, 33(8), 503-513. https://doi.org/10.1002/minf.201300161.